Journal of Organometallic Chemistry, 429 (1992) 187–205
Elsevier Sequoia S.A., Lausanne
JOM 22449

Cluster chemistry

LXXXI *. Reactions of $Ru_3(\mu\text{-dppm})(CO)_{10}$ with $C_2(CO_2Me)_2$. X-Ray structures of $Ru_3\{\mu_3\text{-}C_4(CO_2Me)_4\}(\mu\text{-dppm})(CO)_6$, $Ru_3(\mu\text{-H})_2\{\mu_3\text{-}C_2(CO_2Me)_2\}(\mu\text{-dppm})(CO)_7$ and $Ru_4(\mu_3\text{-H})\{\mu_4\text{-}C_2(CO_2Me)_2\}\text{-}\{\mu\text{-}PPh_2CH_2PPh(C_6H_4)\}(CO)_9$

Michael I. Bruce, Paul A. Humphrey

Jordan Laboratories, Department of Physical and Inorganic Chemistry, University of Adelaide, Adelaide, South Australia 5001 (Australia)

Hiroshi Miyamae **, Brian W. Skelton and Allan H. White

Department of Chemistry, University of Western Australia, Nedlands, Western Australia 6009 (Australia)

(Received July 18, 1991)

Abstract

Several complexes have been obtained from reactions between $Ru_3(\mu\text{-dppm})(CO)_{10}$ and $C_2(CO_2Me)_2$, including $Ru_3\{\mu_3\text{-}C_2(CO_2Me)_2\}(\mu\text{-dppm})(\mu\text{-CO})(CO)_7$ (7), $Ru_3\{\mu_3\text{-}C_4(CO_2Me)_4\}(\mu\text{-dppm})(CO)_6$ (**8**), $Ru_4\{\mu_4\text{-}C_2(CO_2Me)_2\}(\mu\text{-dppm})(CO)_{10}$ (**11**) and $Ru_4(\mu_3\text{-H})\{\mu_4\text{-}C_2(CO_2Me)_2\}\{\mu\text{-}PPh_2CH_2PPh(C_6H_4)\}(CO)_9$ (**10**). A complex related to **10**, containing a $C_4(CO_2Me)_4$ ligand, was obtained directly from $Ru_3(\mu_3\text{-}PPhCH_2PPh(C_6H_4))(CO)_9$ and the alkyne. Ready replacement of CO by 2H occurred in the reaction of **7** with H_2, which afforded $Ru_3(\mu\text{-H})_2\{\mu_3\text{-}C_2(CO_2Me)_2\}(\mu\text{-dppm})(CO)_7$ (**9**). Complexes **8**, **9** and **10** were characterised by single-crystal X-ray studies: in **8**, the $C_4(CO_2Me)_4$ ligand forms a ruthenacyclopentadiene system which interacts in the η^4 mode with the second Ru atom, and via an ester CO group with the third Ru atom. In **9**, the alkyne is attached to the Ru_3 cluster in the $\mu_3\text{-}\eta^2\text{-}\|$ mode, while in **10**, it is incorporated into an octahedral C_2Ru_4 cluster; the metallated dppm ligand bridges an edge of one of the wings of the Ru_4 butterfly. Complexes **10** and **11** were obtained in only 1% and 2% yield, respectively.

Correspondence to: Professor M.I. Bruce, Department of Physical and Inorganic Chemistry, University of Adelaide, PO Box 498, Adelaide, South Australia 5001.

* For Part LXXX, see ref. 1.

** On study leave from Josai University, Japan.

Introduction

The complex $Ru_3(\mu\text{-dppm})(CO)_{10}$ (**1**; Scheme 1) was first reported in 1977 [2] although its molecular structure was not determined until seven years later [3]. Much chemistry of **1** has been reported since. Thus, pyrolysis of **1** afforded $Ru_3\{\mu_3\text{-PPhCH}_2\text{PPh}(C_6H_4)\}(CO)_9$ (**2**), containing a metallated dephenylated dppm ligand, which on heating in CO gave $Ru_3\{\mu\text{-(PPhCH}_2\text{PPh)}C_6H_4\}(CO)_{10}$ (**3**) [4]. Dephenylation of the dppm ligand of **1** also occurred in its reaction with H_2 [4], yielding $Ru_3(\mu\text{-H})\{\mu_3\text{-PPhCH}_2\text{PPh}_2\}(CO)_9$ (**4**). Addition of $K[BH^sBu_3]$ to **1** [5] afforded the dephenylated anion $[Ru_3(\mu_3\text{-PPhCH}_2\text{PPh}_2)(CO)_9]^-$ which could be protonated to yield **4**. Reactions with strong acids, such as $HC_5(CO_2Me)_5$ [6], also gave **2**. Prolonged reaction with H_2 resulted in the formation of $Ru_3(\mu\text{-H})(\mu_3\text{-PPh})(CO)_8(PMePh_2)$ [5]. Substitution of CO in **1** occurs readily with Group 15 ligands [7,8], while addition of HSPh afforded $Ru_3(\mu\text{-H})(\mu\text{-SPh})(\mu\text{-dppm})(CO)_8$ [9]. In most cases, the reactions are clean and afford only one or two products. This stability has encouraged us to look at the reactions of **1** in more detail, particularly those in which $Ru_3(CO)_{12}$ is reported to give complex mixtures or low yields of products. This paper describes some reactions of **1** with $C_2(CO_2Me)_2$; a following contribution will examine its reactions with terminal alkynes.

We have briefly described the reactions between $C_2(CO_2Me)_2$ and $Ru_3(CO)_{12}$ [10] and $Ru_3(CO)_8(PMe_2Ph)_2$ [11]. From the former, the binuclear $Ru_2\{\mu\text{-}C_4(CO_2Me)_4\}(CO)_6$ (**5**) was characterised, and evidence for the formation of complexes with higher oligomers of $C_2(CO_2Me)_2$ was also obtained. The PMe_2Ph complex afforded a rare example of a mono-alkyne complex of the Ru_3 system, $Ru_3\{\mu_3\text{-}C_2(CO_2Me)_2\}(\mu\text{-CO})(CO)_7(PMe_2Ph)_2$ (**6**). Similar unsubstituted complexes, $Ru_3(\mu_3\text{-alkyne})(CO)_{10}$, were recently prepared using $[ppn][Ru_3(\mu\text{-Cl})(CO)_{10}]$ [12] or $Ru_3(CO)_{10}(NCMe)_2$ [13] as intermediates.

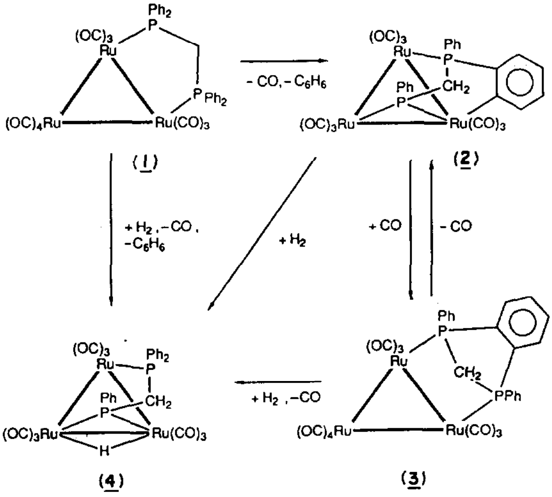

Scheme 1.

Results

The reaction between $C_2(CO_2Me)_2$ and $Ru_3(\mu\text{-dppm})(CO)_{10}$ afforded various products depending on reaction conditions. We have not carried out a detailed survey of the reactions and describe below only the results of those experiments which afforded well-defined products (Scheme 2). Thus, when a 1/1 mixture of **1** and $C_2(CO_2Me)_2$ was heated in refluxing CH_2Cl_2 for three hours, or in refluxing tetrahydrofuran for less than one hour, two major products were isolated in moderate yields (about 30% each). These were characterised as purple $Ru_3\{\mu_3\text{-}C_2(CO_2Me)_2\}(\mu\text{-dppm})(\mu\text{-CO})(CO)_7$ (**7**) and olive-green $Ru_3\{\mu_3\text{-}C_4(CO_2Me)_4\}(\mu\text{-dppm})(CO)_6$ (**8**).

Complex **7** was identified by the usual analytical and spectroscopic methods. The IR spectrum contains ν(CO) bands for both terminal and bridging CO ligands. The ^1H NMR spectrum contains two singlets at δ 3.39 and 3.61, assigned to inequivalent OMe groups, while the CH_2 protons of the μ-dppm ligand give part of an ABXY pattern (two multiplets) at δ 4.85 and 5.50. The FAB mass spectrum contained a pseudo-molecular ion at m/z 1054 corresponding to $[M-H]^+$ derived from an octacarbonyl cluster; this ion fragmented by competitive loss of CO, OMe and $C_2(CO_2Me)_2$. A structure consistent with these data is shown in **7**, in which a closed triangular Ru_3 cluster has one edge bridged by CO and another by the dppm ligand. The $C_2(CO_2Me)_2$ is bonded in the usual $\mu_3\text{-}\eta^2\text{-}\|$ mode, with the C–C bond being approximately parallel to the Ru-Ru edge bridged by the CO ligand. This feature is similar to that found in **6**, but in the latter, the two PMe_2Ph

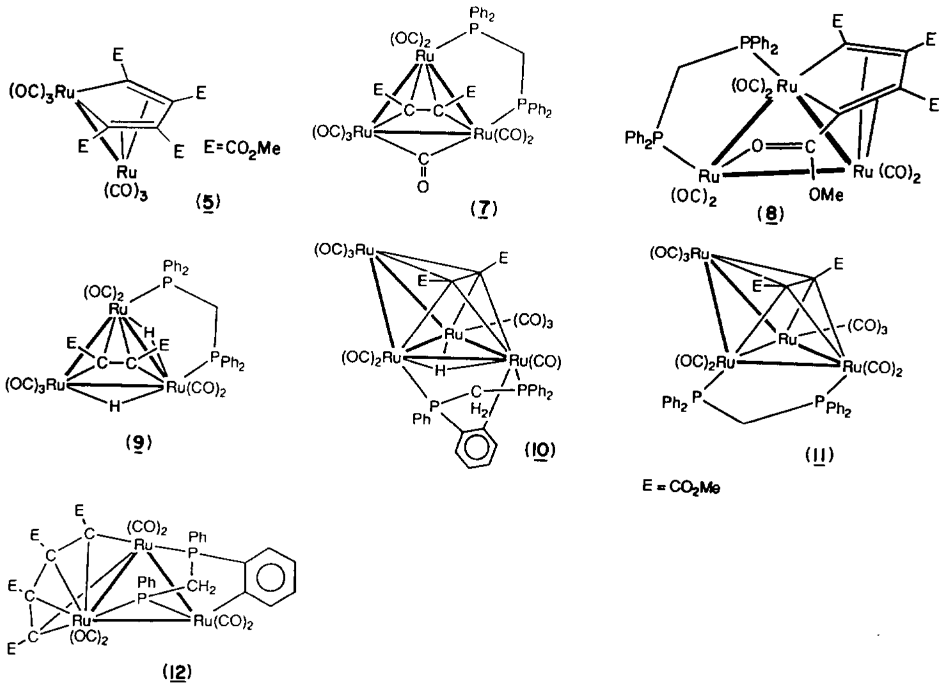

Scheme 2.

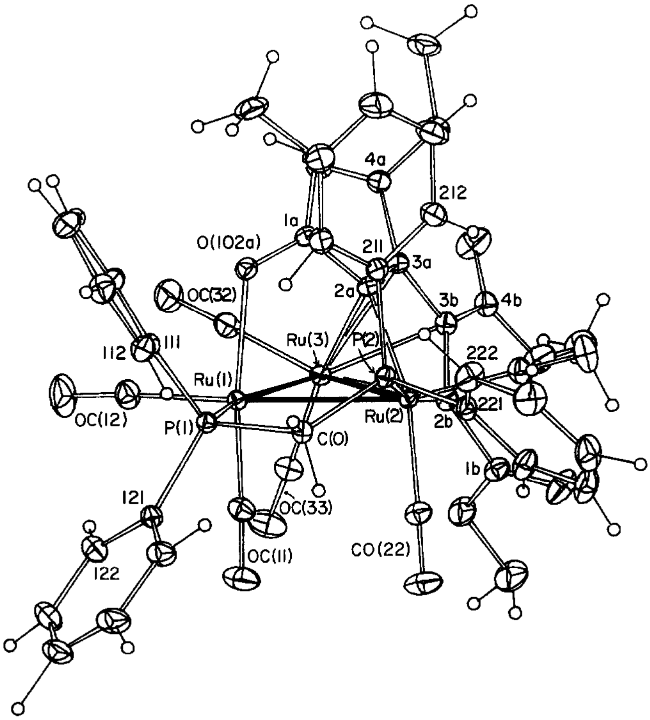

Fig. 1. Computer-generated plot of a molecule of $Ru_3\{\mu_3\text{-}C_4(CO_2Me)_4\}(\mu\text{-dppm})(CO)_6$ (**8**), showing atom numbering scheme. Non-hydrogen atoms are shown with 20% thermal ellipsoids; hydrogen atoms have arbitrary radii of 0.1 Å.

ligands are attached to the two ruthenium atoms σ-bonded to the alkyne and bridged by the CO ligand. In the present case, we suggest that the asymmetric disposition of the dppm, required by the NMR spectroscopic data, results from a minimisation of steric interference of the Ph groups with the other ligands present. Each Ru atom achieves the required 18-electron count in **7**.

The second product, **8**, was also prepared by a reaction of **1** with more than two equivalents of $C_2(CO_2Me)_2$ (72%), or from **7** and further $C_2(CO_2Me)_2$ (79%). The presence of two $C_2(CO_2Me)_2$ moieties was shown by analytical and spectroscopic data. Six ν(CO) bands are found in the solution IR spectrum of **8**, while the ^1H NMR spectrum contained four singlets at δ 2.97, 3.78, 3.79 and 3.80, assigned to four inequivalent OMe groups. The large separation of one of these from the other three is notable. The CH_2 protons are found at δ 7.73 and 5.32 as two doublets of triplets. A molecular ion in the FAB mass spectrum at m/z 1141 loses up to six CO groups, with some further fragmentation occurring readily by loss of $C_2(CO_2Me)_2$ units. The asymmetry of this cluster was not readily accommodated in simple fashion and the molecular structure was determined by X-ray crystallography.

Molecular structure of $Ru_3\{\mu_3\text{-}C_4(CO_2Me)_4\}(\mu\text{-dppm})(CO)_6$ *(8)*

The molecular structure of $Ru_3\{\mu_3\text{-}C_4(CO_2Me)_4\}(\mu\text{-dppm})(CO)_6$ is shown in Fig. 1 and selected bond parameters are collected in Table 1. The molecule

Table 1

Selected bond lengths (Å) and angles (deg.) for $Ru_3\{\mu_3\text{-}C_4(CO_2Me)_4\}(\mu\text{-dppm})(CO)_6$ (**8**)

Ru(1)–Ru(2)	2.8633(6)	Ru(3)–C(3b)	2.292(2)
Ru(1)–Ru(3)	2.6977(5)	Ru(3)–C(2a)	2.220(1)
Ru(2)–Ru(3)	2.7389(4)	Ru(3)–C(2b)	2.171(2)
Ru(1)–P(1)	2.3152(6)	P(1)–C(0)	1.836(2)
Ru(2)–P(2)	2.3687(5)	P(2)–C(0)	1.842(2)
Ru(1)–O(102a)	2.187(1)	O(102a)–C(1a)	1.240(2)
Ru(2)–C(2a)	2.115(2)	C(2a)–C(3a)	1.418(3)
Ru(2)–C(2b)	2.116(2)	C(3a)–C(3b)	1.439(2)
Ru(3)–C(3a)	2.250(2)	C(2b)–C(3b)	1.419(3)
Ru(1)–Ru(2)–P(2)	80.53(1)	C(2a)–Ru(2)–C(2b)	75.66(7)
Ru(2)–Ru(1)–P(1)	102.65(1)	Ru(1)–O(102a)–C(1a)	113.2(1)
Ru(1)–P(1)–C(0)	107.08(5)	Ru(2)–C(2a)–C(3a)	116.7(1)
Ru(2)–P(2)–C(0)	118.76(5)	Ru(2)–C(2b)–C(3b)	116.9(1)
		C(2a)–C(3a)–C(3b)	114.8(2)
P(1)–C(0)–P(2)	113.1(1)	C(3a)–C(3b)–C(2b)	113.2(1)
Ru–CO	range 1.834–1.919(2), av. 1.881 Å		
C–O	range 1.129–1.148(3), av. 1.14 Å		
P–C(Ph)	range 1.824–1.845(2), av. 1.832 Å.		

consists of a closed triangle of three ruthenium atoms [Ru(1)–Ru(2) 2.8633(6), Ru(2)–Ru(3) 2.7389(4), Ru(1)–Ru(3) 2.6977(5) Å] each of which bears two terminal CO groups. The dppm ligand bridges the Ru(1)–Ru(2) bond [Ru(1)–P(1) 2.3152(6), Ru(2)–P(2) 2.3687(5) Å]. A $C_4(CO_2Me)_4$ ligand is attached to Ru(2) via two σ bonds [Ru(2)–C(2a) 2.115(2), Ru(2)–C(2b) 2.116(2) Å], to Ru(3) by an η^4 interaction with the C_4 (diene) system [Ru(3)–C(2a,3a) 2.220(1), 2.250(2), Ru(3)–C(2b,3b) 2.171(2), 2.292(2) Å] and to Ru(1) by an *O*-donor bond from the ester CO group [Ru(1)–O(102a) 2.187(1) Å]. The torsion angle τ(C(2a,3a,3b,2b)) is 5.8(2)°, while τ(C(1,2,3,4)) are 9.6(2) and 4.9(3)° for sections a, b, respectively. This unusual geometry explains the asymmetry of the $C_4(CO_2Me)_4$ group suggested by the NMR spectrum, in particular the single CO_2Me group at δ 2.97. It also allows the Ru_3 cluster to become electron-precise.

In **1**, the Ru–Ru bond lengths range from 2.834–2.860(1) Å, the shortest being that bridged by the dppm ligand. In **8**, this is the longest bond. An alternative view of **8** is related to the structure of $Ru_2\{\mu\text{-}C_4(CO_2Me)_4\}(CO)_6$, referred to above [10]. In the related $Fe_2(\mu\text{-}C_4R_4)(CO)_6$ structures a CO group bridges the Fe–Fe bond, although this feature is absent in the ruthenium derivative. However, conceptual replacement of this μ-CO group in the ruthenium complex by the isolobal $Ru(CO)_3(L)$ (L = P of dppm) group leads to **8**. In accord with this suggestion, the Ru–Ru distance bridged by the diene is similar to that found in $Ru_2\{\mu\text{-}C_4(CO_2Me)_4\}(CO)_6$ [2.734(2), 2.753(2) Å in the crystallographically distinct molecules [10]].

We also carried out a reaction between a 1/1 mixture of **1** and $C_2(CO_2Me)_2$ in refluxing tetrahydrofuran for 18 h. This gave a complex mixture of products, including **2** (18%), **7** (1%) and **8** (22%), together with a fourth product, characterised as orange $Ru_3(\mu\text{-H})_2\{\mu_3\text{-}C_2(CO_2Me)_2\}(\mu\text{-dppm})(CO)_7$ (**9**) (1%). This complex was prepared in higher yield (77%) by direct hydrogenation of **7** in refluxing

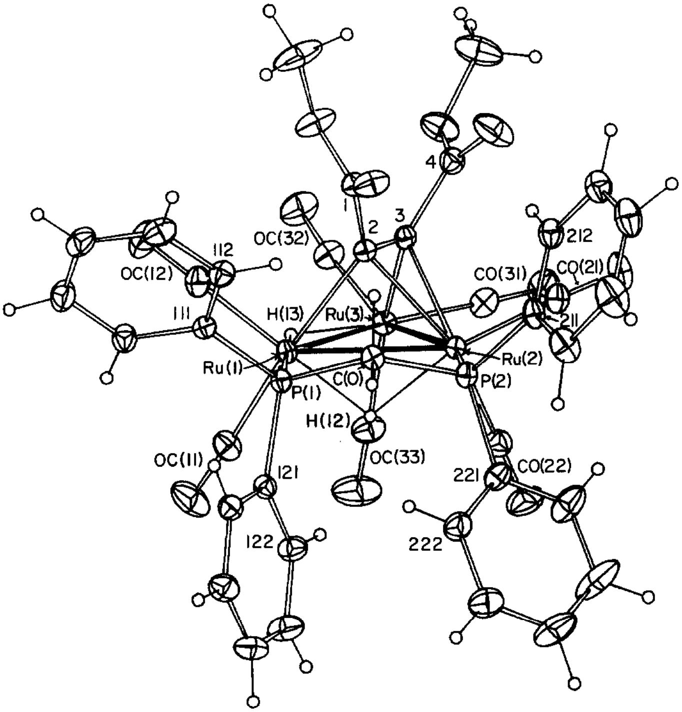

Fig. 2. Computer-generated plot of a molecule of $Ru_3(\mu\text{-}H)_2\{\mu_3\text{-}C_2(CO_2Me)_2\}(\mu\text{-}dppm)(CO)_7$ (**9**), showing atom numbering scheme. Non-hydrogen atoms are shown with 20% thermal ellipsoids; hydrogen atoms have arbitrary radii of 0.1 Å.

CH_2Cl_2. It was initially characterised from analytical and spectroscopic data. The IR $\nu(CO)$ spectrum contained only terminal CO bands, while the formulation was confirmed by the FAB mass spectrum, with a molecular ion at m/z 1029 which fragmented by loss of CO, OMe and CO_2Me groups. In the ^1H NMR spectrum, two Ru-H signals occur at δ − 14.9 (doublet) and −19.2 (triplet), with coupling to ^{31}P of 14 and 39 Hz, respectively. The OMe resonances are inequivalent at δ 3.46 and 3.76, while the CH_2 protons of the dppm ligand are found at δ 3.56 and 4.49 (part of ABXY pattern). These data allowed the assignment of structure **9** to this cluster, but the rarity of mono-alkyne-Ru_3 clusters encouraged us to seek confirmation by means of an X-ray study.

Molecular structure of $Ru_3(\mu\text{-}H)_2\{\mu_3\text{-}C_2(CO_2Me)_2\}(\mu\text{-}dppm)(CO)_7$ (9)

The molecular structure of **9** is shown in Fig. 2, with selected bond lengths and angles given in Table 2. As expected, a triangle of ruthenium atoms is spanned by the $C_2(CO_2Me)_2$ ligand in the $\mu_3\text{-}\eta^2\text{-}\|$ mode, as found previously in **6**. One Ru–Ru bond is bridged by the dppm ligand, the two Ru atoms each bearing two CO groups; the third Ru has three CO groups. The hydride atoms were located and refined in the structural study, and their locations are consistent with the NMR data. One H is coupled equally to the two ^{31}P nuclei, suggesting that it bridges Ru(1)–Ru(2). This bond, at 2.836(1) Å, is longer than that joining the two phosphine-substituted Ru atoms in **6** [2.817(1) Å]. The other hydrogen atom,

Table 2

Selected bond lengths (Å) and angles (deg.) for $Ru_3(\mu\text{-}H)_2\{\mu_3\text{-}C_2(CO_2Me)_2\}(\mu\text{-dppm})(CO)_7$ (**9**)

Ru(1)-Ru(2)	2.836(1)	P(1)-C(0)	1.827(4)
Ru(1)-Ru(3)	2.9764(8)	P(2)-C(0)	1.834(4)
Ru(2)-Ru(3)	2.7491(7)	C(1)-C(2)	1.483(5)
Ru(1)-P(1)	2.332(1)	C(2)-C(3)	1.398(6)
Ru(2)-P(2)	2.351(1)	C(3)-C(4)	1.489(8)
Ru(1)-C(2)	2.122(4)	Ru(1)-H(12)	1.77(4)
Ru(2)-C(2)	2.216(4)	Ru(1)-H(13)	1.75(4)
Ru(2)-C(3)	2.241(5)	Ru(2)-H(12)	1.83(5)
Ru(3)-C(3)	2.037(4)	Ru(3)-H(13)	1.74(4)
Ru(2)-Ru(1)-P(1)	92.53(4)	Ru(2)-C(3)-Ru(3)	79.8(1)
Ru(1)-Ru(2)-P(2)	94.29(4)	Ru(1)-C(2)-C(3)	109.8(3)
Ru(1)-P(1)-C(0)	114.1(2)	Ru(3)-C(3)-C(2)	114.6(3)
Ru(2)-P(2)-C(0)	112.0(1)		
P(1)-C(0)-P(2)	116.6(2)	C(1)-C(2)-C(3)	121.6(4)
Ru(1)-C(2)-Ru(2)	81.6(1)	C(2)-C(3)-C(4)	118.4(3)
Ru-CO	range 1.870-1.958(5), av. 1.902 Å		
C-O	range 1.128-1.138(6), av. 1.130 Å		
P-C(Ph)	range 1.819-1.829(4), av. 1.823 Å.		

coupled to only one ^{31}P nucleus, bridges the longest bond, Ru(1)-Ru(3); the location of the H atom on this bond is accompanied by the splaying of CO(11) and CO(33) [C(11)-Ru(1)-C(12) 94.5(2), C(32)-Ru(3)-C(33) 101.4(2)°]. H(12,13) lie 1.07(5) and 0.02(4) Å, respectively, out of the Ru_3 plane, i.e. H(13) is coplanar with the three metal atoms.

Comparison of the bonding parameters for the $C_2(CO_2Me)_2$ ligand reveals little difference between this ligand in complexes **6** and **9**. There is a slightly greater degree of asymmetry in the latter, *e.g.* the Ru(2)-C(2, 3) distances differ by 0.02_5 Å in **9** compared with 0.01 Å in **6**, and there is a difference of 0.08_5 Å in the two Ru-C(alkyne) σ bonds in **9**, whereas in **6** they are experimentally equal.

As also found for **6**, the Ru-CO bonds *trans* to the σ-bonded alkyne carbons [Ru(1)-C(11) 1.919(5), Ru(3)-C(33) 1.958(5) Å] are considerably longer than the other Ru-CO bonds on these atoms [Ru(1)-C(12) 1.886(4), Ru(3)-C(31, 32) 1.887, 1.886(5) Å].

Two other products isolated in low yields from the prolonged reaction in tetrahydrofuran were found to be tetranuclear ruthenium clusters. The first was an orange complex identified by an X-ray study as $Ru_4(\mu_3\text{-}H)\{\mu_4\text{-}C_2(CO_2Me)_2\}\{\mu\text{-}PPh_2CH_2PPh(C_6H_4)\}(CO)_9$ (**10**) and was isolated in 1% yield. The IR spectrum contained only terminal ν(CO) bands, while the FAB spectrum contained a pseudo-molecular ion at *m/z* 1183, which decomposed by loss of CO and $C_2(CO_2Me)_2$.

Molecular structure of $Ru_4(\mu_3\text{-}H)\{\mu_4\text{-}C_2(CO_2Me)_2\}\{\mu\text{-}PPh_2CH_2PPh(C_6H_4)\}(CO)_9$ *(10)*

Figure 3 depicts a molecule of **10**, and Table 3 contains some structural parameters. The structure is based on the *closo*-octahedral C_2Ru_4 cluster, alterna-

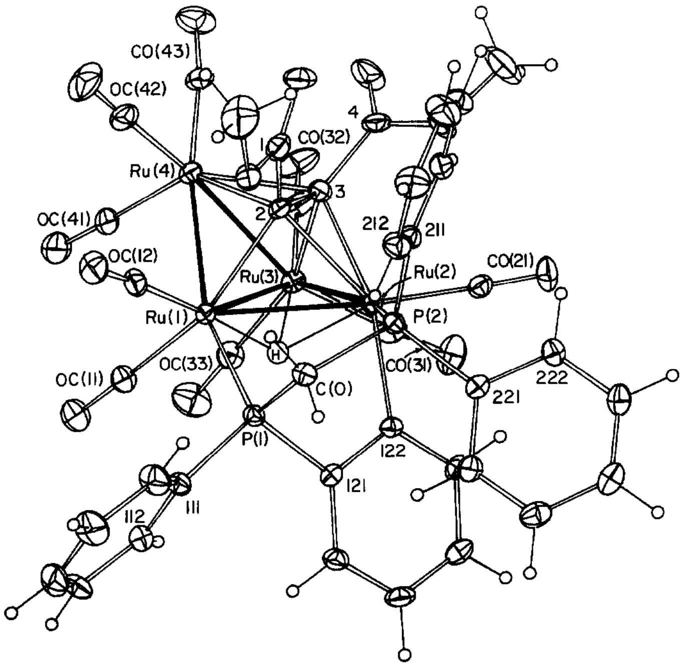

Fig. 3. Computer-generated plot of a molecule of $Ru_4(\mu_3\text{-}H)\{\mu_4\text{-}C_2(CO_2Me)_2\}\{\mu\text{-}PPh_2CH_2PPh(C_6H_4)\}(CO)_9$ (**10**), showing atom numbering scheme. Non-hydrogen atoms are shown with 20% thermal ellipsoids; hydrogen atoms have arbitrary radii of 0.1 Å.

Table 3

Selected bond lengths (Å) and angles (deg.) for $Ru_4(\mu_3\text{-}H)\{\mu_4\text{-}C_2(CO_2Me)_2\}\{\mu\text{-}PPh_2CH_2PPh(C_6H_4)\}(CO)_9$ (**10**)

Ru(1)–Ru(2)	2.807(1)	Ru(4)–C(3)	2.218(8)
Ru(1)–Ru(3)	2.942(1)	Ru(2)–C(122)	2.073(7)
Ru(1)–Ru(4)	2.723(1)	Ru(1)–H	1.74(6)
Ru(2)–Ru(3)	2.851(1)	Ru(2)–H	2.07(6)
Ru(3)–Ru(4)	2.739(1)	Ru(3)–H	1.86(6)
Ru(1)–P(1)	2.309(2)	P(1)–C(0)	1.834(8)
Ru(2)–P(2)	2.268(2)	P(2)–C(0)	1.830(8)
Ru(1)–C(2)	2.146(8)	P(1)–C(121)	1.812(7)
Ru(2)–C(2)	2.230(7)	C(1)–C(2)	1.50(1)
Ru(2)–C(3)	2.317(8)	C(2)–C(3)	1.44(1)
Ru(3)–C(3)	2.139(7)	C(3)–C(4)	1.49(1)
Ru(4)–C(2)	2.257(7)	C(121)–C(122)	1.42(1)
Ru(2)–Ru(1)–P(1)	71.81(6)	Ru(2)–P(2)–C(0)	105.1(2)
Ru(1)–Ru(2)–P(2)	98.81(6)	Ru(2)–C(122)–C(121)	116.1(5)
Ru(1)–Ru(2)–C(122)	95.8(2)	P(1)–C(0)–P(2)	106.2(4)
Ru(3)–Ru(2)–C(122)	101.2(2)	P(1)–C(121)–C(122)	112.5(5)
Ru(1)–P(1)–C(0)	111.4(2)		
Ru–CO	range 1.838–1.915(8), av. 1.890 Å		
C–O	range 1.13–1.16(1), av. 1.14 Å		
P–C(Ph)	range 1.812–1.817(8), av. 1.814 Å.		

tively on an Ru_4 butterfly containing a μ_4-η^2-$C_2(CO_2Me)_2$ ligand. A hydrogen atom, located and refined in the X-ray study, caps the Ru(1)–Ru(2)–Ru(3) face, lying outside it by 0.88(6) Å, while the *ortho*-metallated dppm ligand bridges the Ru(1)–Ru(2) edge. Coordination of the rutheniums is completed by nine CO ligands, distributed three to each of Ru(3) and Ru(4), two to Ru(1) and one to Ru(2). The Ru-Ru bond lengths range from 2.723(1) to 2.942(1) Å, the longest being the hinge of the butterfly. The presence of the μ_3-H atom causes a marked enlargement of the capped Ru(1)–Ru(2)–Ru(3) face compared with the non-capped Ru(1)–Ru(3)–Ru(4) face; the non-hinge Ru–Ru distances are 2.807, 2.851(1) Å in the H-capped face, 2.723, 2.739(1) Å in the non-capped face. The Ru(1,2,3)/Ru(1,3,4) interplanar dihedral is 115.91(3)°.

The metallated dppm ligand is bonded to only two Ru atoms. The two P atoms are attached to Ru(1) and Ru(2) [Ru(1)–P(1) 2.309(2), Ru(2)–P(2) 2.268(2) Å], while the C_6H_4 group attached to P(1) forms a σ bond to Ru(2) [Ru(2)–C(122) 2.073(7) Å]. This ligand has been found in two other clusters: **2** and the unsaturated osmium derivative $Os_3(\mu$-$H)\{\mu_3$-$PPh_2CH_2PPh(C_6H_4)\}(CO)_8$ [14]; in the latter, however, the C_6H_4 group bridges an Os-Os bond.

The $C_2(CO_2Me)_2$ ligand is bonded in a 2σ, 2π mode to all four Ru atoms. Bonds to the hinge atoms [Ru(1)–C(2) 2.146(8), Ru(3)–C(3) 2.139(8) Å] are shorter than to the wing-tip atoms [2.218–2.317(8) Å]; the longest of the latter is *trans* to the Ru–C(Ar) σ bond, reflecting the strong *trans* influence of the latter. The central C–C bond length is 1.44(1) Å.

Electron counting for this cluster results in a two-electron deficiency, although consideration of the *closo*-octahedral C_2Ru_4 core by polyhedral skeletal electron pair counting rules [15] results in a normal electron count (66 e) for this species.

A second tetranuclear complex was identified as $Ru_4\{\mu_4$-$C_2(CO_2Me)_2\}(\mu$-dppm$)(CO)_{10}$ (**11**) by analytical and spectroscopic techniques. This compound was isolated in only 2% yield, and X-ray quality crystals were not obtained. The IR spectrum contains eight terminal ν(CO) bands and the FAB mass spectrum has a molecular ion at *m/z* 1212, which fragments by loss of CO and OMe groups. In the ^{1}H NMR spectrum, two singlets are found at δ 3.03 and 3.79 for non-equivalent OMe groups and the two doublets of triplets for the CH_2 protons of the dppm ligand are at δ 4.75 and 4.97. These data are consistent with the illustrated structure **11**, consisting of a C_2Ru_4 core, with the dppm ligand bridging one of the (non-hinge) Ru–Ru edges.

Reaction between $Ru_3\{\mu_3$-$PPhCH_2PPh(C_6H_4)\}(CO)_9$ and $C_2(CO_2Me)_2$

We have also examined the reaction between $C_2(CO_2Me)_2$ and the cluster $Ru_3\{\mu_3$-$PPhCH_2PPh(C_6H_4)\}(CO)_9$ (**4**) which contains a metallated, dephenylated dppm ligand. A dark green complex was isolated from tetrahydrofuran and identified as $Ru_3\{\mu_3$-$PPhCH_2PPh(C_6H_4)\}\{\mu$-$C_4(CO_2Me)_4\}(CO)_6$ (**12**) by conventional analytical and spectroscopic methods. There are six terminal ν(CO) bands in the IR spectrum of **12**; a Nujol mull exhibits strong ν(CO) and ν(COO) bands at lower wavenumbers. The ^{1}H NMR spectrum contains four singlet resonances between δ 3.45 and 3.91, assigned to the CO_2Me protons, while the CH_2 group resonates as a multiplet between δ 2.5 and 3.0, which can be analysed as part of an ABXY spin system. The FAB mass spectrum contains a molecular ion at *m/z* 1063, which decomposed by loss of CO and $C_2(CO_2Me)_2$ groups.

The likely structure of **12** is similar to that found for **8** above, with the difference that the CO_2Me group is not coordinated to a metal atom. Both the modified dppm ligand and the $C_4(CO_2Me)_4$ ligands donate six electrons to the cluster, which with the six CO groups then achieves a 48-electron count. This is supported by the ^1H NMR spectrum, which does not contain the deshielded resonance at δ *ca.* 3 which we have assigned to the coordinated CO_2Me group. The structure is also similar to that of the related complex obtained from HC_2Ph, which has been characterised by X-ray crystallography [16].

Discussion

The reactions between **1** and $C_2(CO_2Me)_2$ proceed readily in polar solvents such as CH_2Cl_2 or tetrahydrofuran. After short reaction times, trinuclear products can be isolated; prolonged reaction results in the formation of small amounts of tetranuclear complexes. The X-ray structural studies have shown that initial formation of a complex containing one molecule of the alkyne, attached in the common μ_3-η^2-|| mode, occurs. Excess alkyne reacts with this to form a metallacyclopentadiene derivative, and it is reasonable to assume that the formation of the tetranuclear clusters results from addition of '$Ru(CO)_3$' to the mono-alkyne species. The formation of **10** may result from thermal degradation of the dppm ligand in **11**, with transfer of H to the cluster, as found for the precursor **1**.

Dimerisation of $C_2(CO_2Me)_2$ has been observed before in the reaction with $Ru_3(CO)_{12}$ [10], which afforded a binuclear metallacyclopentadiene complex; other oligomers have been identified in related reactions, a trimer being present in $Ru_3\{C_2(CO_2Me)_2\}_3(CO)_6(PMe_2Ph)_2$ [11] and a tetramer in $Ru_3\{C_2(CO_2Me)_2\}_4(CO)_7$ [10]. Unfortunately, these two complexes have not yielded X-ray quality crystals so far; investigations are proceeding.

In **9**, one of the ester CO groups is also coordinated to the cluster. This is not uncommon in ruthenium cluster chemistry. Previously characterised examples include $Ru_3(\mu\text{-}H)_2\{\mu_3\text{-}CHC(O)Me\}(CO)_9$ (**13**) [17] and the butterfly cluster $Ru_4\{\mu_4\text{-}HC_2CMe_2NHCOC_6H_9\}(CO)_{11}$ (**14**) [18].

Comparison of the molecular structures of analogous ruthenium and osmium complexes containing the same μ_3-η^2-||-alkyne showed that the alkyne was more symmetrically bonded in the Ru complexes [13]. In both **6** and **9**, we have found that the degree of distortion from symmetrical attachment is small. Even the presence of the dppm ligand bridging one edge of the Ru_3 cluster has very little effect on the bonding of the alkyne.

The trinuclear complexes described in this paper are very reactive, as indicated by the complex mixture of products obtained from the prolonged reactions referred to above. This reactivity is a function of the phosphine and alkyne substituents. We shall describe elsewhere their reactions with a variety of reagents. However, in the present account, we have shown that ready coupling of a second molecule of alkyne occurs on the Ru_3 clusters. There is ample precedent for this type of reaction, the most recent being studies of reactions between binuclear iron derivatives of diazabutadienes and various alkynes affording related ferracyclopentadiene complexes [19]. These reactions have converted the alkyne from a μ_3-bridging mode to a μ_2-diene position above one Ru–Ru edge. Only in the case of **8** was a μ_3-ligand found, but even in this case it is not via the C_4 skeleton, which remains above the edge, but through a functional group (CO_2Me) attached to the C_4 unit. It seems that this type of reaction potentially frees a site on the third metal for coordination of another small molecule, which perhaps could enable further coupling to take place.

The mode of attachment of the metallated dppm ligand in **10** deserves further comment. In the previously characterised example, the ligand, containing a CP_2 donor set, spans the Ru_3 triangle, the cluster-bound H atom bridging an edge [4]. In **10**, the ligand bridges an Ru–Ru edge, orthogonal coordination positions on Ru(2) being occupied by the P and C atoms, so that the two phosphorus atoms are also orthogonal across the Ru–Ru bond. The reasons for these differences are not clear at present, but can probably be attributed to the unusual electronic requirements of the C_2Ru_4 cluster.

Conclusions

Reactions between $Ru_3(\mu\text{-dppm})(CO)_{10}$ and $C_2(CO_2Me)_2$ probably proceed via initial formation of a reactive μ_3-η^2-alkyne complex (**7**); further reaction occurs readily to give a dimer of the alkyne attached to two of the Ru atoms by the C_4 system and to the third by the ester carbonyl oxygen in **8**. Other minor products include tetranuclear derivatives containing octahedral C_2Ru_4 cores. This chemistry differs from that found for $Ru_3(CO)_{12}$ in giving higher yields and fewer products; the reactions proceed under milder conditions. Ready replacement of one CO in **7** by 2H was achieved in its reaction with H_2; a complex containing a metallated dppm ligand reacted with $C_2(CO_2Me)_2$ to give a product analogous to **8**. The alkyne in **7** is evidently very reactive and further studies of its C–C bond forming reactions are in progress.

Experimental

General conditions

All reactions were carried out under dry, high purity nitrogen using standard Schlenk techniques. Solvents were dried and distilled before use. Elemental analyses were by the Canadian Microanalytical Service, Delta, British Columbia. Preparative TLC was carried out on glass plates (20 × 20 cm) coated with silica gel (Merck 60 GF_{254}, 0.5 mm thick).

Complexes **1** [20] and **4** [6] were prepared by published methods. $Me_3NO.2H_2O$ (Aldrich) was dehydrated by sublimation (100°C/0.1 mm Hg); $C_2(CO_2Me)_2$ was obtained from Heinrich Mach Nachf., Illertissen, Germany, and was distilled before use. The following instrumentation was used. IR: Perkin-Elmer 683 double beam, NaCl optics; 1720FT; NMR: Bruker CXP300 (^1H NMR at 300.13 MHz, ^{13}C NMR at 75.47 MHz). Spectra recorded in non-deuterated solvents used an external concentric tube containing D_2O for field lock. FAB MS: VG ZAB 2HF (FAB MS, using 3-nitrobenzyl alcohol as matrix, exciting gas Ar, FAB gun voltage 7.5 kV, current 1 mA, accelerating potential 7 kV).

Reactions between $Ru_3(\mu\text{-dppm})(CO)_{10}$ and $C_2(CO_2Me)_2$

(a) A mixture of $Ru_3(\mu\text{-dppm})(CO)_{10}$ (243 mg, 0.251 mmol) and $C_2(CO_2Me)_2$ (40 mg, 0.28 mmol) in CH_2Cl_2 (15 ml) was refluxed for 3 h. After removal of solvent,

Table 4

Non-hydrogen atomic coordinates and isotropic thermal parameters for $Ru_3\{\mu_3\text{-}C_4(CO_2Me)_4\}(\mu\text{-}dppm)(CO)_6$ (**8**)

Atom	x	y	z	U_{eq} (Å^2)
Ru(1)	0.67182(0)	0.01616(1)	0.75121(1)	0.02420(4)
Ru(2)	0.82320(0)	−0.06934(1)	0.72809(1)	0.02209(3)
Ru(3)	0.72091(0)	−0.22069(1)	0.79359(1)	0.02458(4)
C(11)	0.6882(1)	−0.0254(2)	0.9289(2)	0.0413(7)
O(11)	0.6958(1)	−0.0479(2)	1.0400(2)	0.0698(8)
C(12)	0.5711(1)	0.0251(2)	0.7766(2)	0.0491(9)
O(12)	0.5113(1)	0.0221(2)	0.8021(3)	0.090(1)
C(21)	0.9195(1)	−0.0994(2)	0.6619(2)	0.0381(6)
O(21)	0.97602(9)	−0.1195(2)	0.6238(2)	0.0648(8)
C(22)	0.8504(1)	−0.0585(2)	0.8876(2)	0.0426(7)
O(22)	0.8659(1)	−0.0562(2)	0.9870(2)	0.082(1)
C(32)	0.6256(1)	−0.2267(2)	0.7566(2)	0.0448(8)
O(32)	0.56685(9)	−0.2302(2)	0.7351(2)	0.075(1)
C(33)	0.6975(1)	−0.2922(2)	0.9750(2)	0.0418(7)
O(33)	0.6809(1)	−0.3369(2)	1.0835(2)	0.0715(8)
P(1)	0.66877(2)	0.22278(4)	0.69977(4)	0.0275(1)
C(111)	0.61669(9)	0.3333(2)	0.5551(2)	0.0314(5)
C(112)	0.6245(1)	0.4566(2)	0.5066(2)	0.0403(7)
C(113)	0.5873(1)	0.5400(2)	0.3940(2)	0.0489(8)
C(114)	0.5409(1)	0.5017(2)	0.3302(2)	0.0564(9)
C(115)	0.5317(1)	0.3822(2)	0.3781(2)	0.0554(9)
C(116)	0.5693(1)	0.2964(2)	0.4909(2)	0.0423(7)
C(121)	0.63849(9)	0.2833(2)	0.8286(2)	0.0328(6)
C(122)	0.5857(1)	0.2335(2)	0.9183(2)	0.0446(7)
C(123)	0.5581(1)	0.2840(2)	1.0106(2)	0.0595(9)
C(124)	0.5830(2)	0.3849(2)	1.0127(2)	0.062(1)
C(125)	0.6351(2)	0.4339(2)	0.9252(2)	0.059(1)
C(126)	0.6638(1)	0.3840(2)	0.8330(2)	0.0460(8)
C(0)	0.76278(9)	0.2520(1)	0.6665(2)	0.0298(5)
P(2)	0.82065(2)	0.14265(4)	0.60629(4)	0.0270(1)
C(211)	0.80280(9)	0.1938(2)	0.4282(2)	0.0329(6)
C(212)	0.8400(1)	0.1233(2)	0.3608(2)	0.0482(8)
C(213)	0.8306(2)	0.1604(3)	0.2246(2)	0.070(1)
C(214)	0.7850(2)	0.2665(3)	0.1551(2)	0.075(1)
C(215)	0.7482(1)	0.3370(2)	0.2201(2)	0.062(1)
C(216)	0.7574(1)	0.3011(2)	0.3570(2)	0.0450(7)
C(221)	0.90755(9)	0.1980(2)	0.5991(2)	0.0336(6)
C(222)	0.9174(1)	0.3091(2)	0.5009(2)	0.0512(8)
C(223)	0.9817(1)	0.3551(3)	0.4912(3)	0.067(1)
C(224)	1.0369(1)	0.2896(3)	0.5805(3)	0.066(1)
C(225)	1.0280(1)	0.1812(2)	0.6792(3)	0.062(1)
C(226)	0.9633(1)	0.1347(2)	0.6904(2)	0.0484(8)
C(1a)	0.70835(9)	−0.0228(1)	0.5052(2)	0.0300(5)
O(101a)	0.70565(8)	−0.0247(1)	0.3861(1)	0.0447(5)
O(102a)	0.66521(7)	0.0511(1)	0.5393(1)	0.0349(4)
C(101a)	0.6472(2)	0.0596(3)	0.2984(2)	0.071(1)
C(2a)	0.76383(9)	−0.1111(1)	0.5970(2)	0.0278(5)
C(3a)	0.77572(9)	−0.2345(1)	0.6083(2)	0.0295(5)
C(4a)	0.7413(1)	−0.2752(2)	0.5138(2)	0.0353(6)
O(401a)	0.78756(8)	−0.2775(1)	0.4169(1)	0.0481(6)
O(402a)	0.68104(8)	−0.2968(2)	0.5216(2)	0.0542(7)

Table 4 (continued)

Atom	x	y	z	U_{eq} (Å^2)
C(401a)	0.7600(2)	−0.3068(3)	0.3135(3)	0.068(1)
C(1b)	0.8881(1)	−0.3326(2)	0.9219(2)	0.0376(6)
O(101b)	0.85446(9)	−0.4018(2)	1.0271(1)	0.0583(6)
O(102b)	0.95114(9)	−0.3240(2)	0.9214(2)	0.0641(7)
C(101b)	0.9014(2)	−0.4791(3)	1.1396(3)	0.078(1)
C(2b)	0.83878(9)	−0.2627(1)	0.8044(2)	0.0302(5)
C(3b)	0.82056(9)	−0.3180(1)	0.7192(2)	0.0311(5)
C(4b)	0.8411(1)	−0.4488(2)	0.7364(2)	0.0360(6)
O(401b)	0.8918(1)	−0.5085(1)	0.8270(2)	0.0590(7)
O(402b)	0.8153(1)	−0.4950(1)	0.6728(2)	0.0673(8)
C(401b)	0.9149(2)	−0.6365(2)	0.8530(3)	0.062(1)

preparative TLC (acetone/light petroleum 3/7) separated seven bands. Band 2 (red, R_f 0.55) contained $Ru_3(\mu\text{-dppm})(CO)_{10}$ (70 mg, 29%), identified by IR and spot TLC. Band 3 (purple, R_f 0.45) gave purple crystals (from CH_2Cl_2/hexane) of $Ru_3\{\mu_3\text{-}C_2(CO_2Me)_2\}(\mu\text{-dppm})(\mu\text{-CO})(CO)_7$ (**7**) (80 mg, 30%), m.p. 205–207°C. (Found: C, 44.78; H, 2.94; M (mass spectrometry), 1054. $C_{39}H_{28}O_{12}P_2Ru_3$ calc.: C, 44.45; H, 2.68%; M, 1055). IR: ν(CO) (cyclohexane) 2070 vs, 2041 s, 2016 vs, 2002 vs, 1978 m, 1858w (br), 1855 m cm^{-1}. ^{1}H NMR: δ ($CDCl_3$) 3.39 (s, 3H, OMe), 3.61 (s, 3H, OMe), 4.85 (m, part of ABXY system, 1H, CH_2), 5.50 (m, part of ABXY system, 1H, CH_2), 7.37 (m, 20H, Ph). FAB MS: 1054, $[M-H]^+$, 9; 1026, $[M-H-CO]^+$, 63; 996, $[M-H-OMe]^+$, 14; 968, $[M-H-2CO-OMe]^+$, 62; 943, $[M-4CO]^+$, 68; 915, $[M-5CO]^+$, 89; 887, $[M-6CO]^+$, 100; 859, $[M-7CO]^+$, 89; 829, $[M-3CO-C_2(CO_2Me)_2]^+$, 61; 801, $[M-4CO-C_2(CO_2Me)_2]^+$, 47; 772, $[M-5CO-C_2(CO_2Me)_2]^+$, 59. Band 5 (olive-green, R_f 0.18) gave green crystals (from CH_2Cl_2/hexane) of $Ru_3\{\mu_3\text{-}C_4(CO_2Me)_4\}(\mu\text{-dppm})(CO)_6$ (**8**) (92 mg, 32%), m.p. 262 – 266°C. (Found: C, 45.31; H, 2.99; M (mass spectrometry) 1141; $C_{43}H_{34}O_{14}P_2Ru_3$ calc.: C, 45.31; H, 3.01%; M, 1141). IR: ν(CO)(CH_2Cl_2) 2034 m, 2013 vs, 1977 (sh), 1969 s, 1951 m, 1930 w; ν(CO) (Nujol) 2037 s, 2008 vs, 1978 vs, 1971 s, 1950 vs, 1927 m; ν(C=O) 1742 m, 1738 (sh), 1711 s, 1705 (sh); ν(COO) 1261 w, 1219 m, 1211 (sh), 1171 w cm^{-1}. ^{1}H NMR: δ($CDCl_3$) 2.97 (s, 3H, OMe), 3.78 (s, 3H, OMe), 3.79 (s, 3H, OMe), 3.80 (s, 3H, OMe), 4.73 (dt, J(HH) = 15, J(PH) = 11, 1H, CH_2), 5.32 (dt, J(HH) = 15, J(PH) = 11, 1H, CH_2), 7.06–7.91 (m, 20H, Ph). FAB MS: 1141, M^+, 47; 1113, $[M-CO]^+$, 45; 1085, $[M-2CO]^+$, 89; 1057, $[M-3CO]^+$, 83; 1029, $[M-4CO]^+$, 99; 1001, $[M-5CO]^+$, 100; 973, $[M-6CO]^+$, 92; 943, $[M-2CO-C_2(CO_2Me)_2]^+$, 42; 915, $[M-3CO-C_2(CO_2Me)_2]^+$, 94; 857, $[M-2C_2(CO_2Me)_2]^+$, 49.

(b) A mixture of $Ru_3(\mu\text{-dppm})(CO)_{10}$ (175 mg, 0.181 mmol) and $C_2(CO_2Me)_2$ (70 mg, 0.49 mmol) in tetrahydrofuran (15 ml) was refluxed for 40 min, after which time all the $Ru_3(\mu\text{-dppm})(CO)_{10}$ had been consumed (spot TLC). After evaporation to dryness, crystallisation (CH_2Cl_2/MeOH) of the residue afforded olive-green microcrystals of $Ru_3\{\mu_3\text{-}C_4(CO_2Me)_4\}(\mu\text{-dppm})(CO)_6$ (**8**) (149 mg, 72%), identical with the complex prepared in (a) above.

(c) A mixture of $Ru_3(\mu\text{-dppm})(CO)_{10}$ (182 mg, 0.188 mmol) and $C_2(CO_2Me)_2$ (29 mg, 0.204 mmol) in tetrahydrofuran (20 mol) was refluxed for 18 h. Evaporation and separation of the residue by preparative TLC (acetone/light petroleum 3/7)

Table 5

Non-hydrogen atomic coordinates and isotropic thermal parameters for $Ru_3(\mu\text{-}H)_2\{\mu_3\text{-}C_2(CO_2Me)_2\}(\mu\text{-dppm})(CO)_7$ (**9**)

Atom	*x*	*y*	*z*	U_{eq} (Å^2)
Ru(1)	0.23282(2)	−0.00544(3)	1.04028(3)	0.0301(1)
Ru(2)	0.29084(2)	0.04181(3)	0.74465(3)	0.0276(1)
Ru(3)	0.27860(2)	−0.20633(3)	0.87789(3)	0.0326(1)
C(11)	0.2938(3)	−0.0855(4)	1.1759(5)	0.053(2)
O(11)	0.3279(2)	−0.1395(4)	1.2583(4)	0.090(2)
C(12)	0.1457(3)	−0.0221(4)	1.1748(5)	0.052(2)
O(12)	0.0933(2)	−0.0345(4)	1.2543(4)	0.085(2)
C(21)	0.2904(2)	0.0657(4)	0.5554(4)	0.045(2)
O(21)	0.2932(2)	0.0771(3)	0.4393(3)	0.073(2)
C(22)	0.3931(2)	−0.0292(4)	0.7032(5)	0.049(2)
O(22)	0.4544(2)	−0.0731(4)	0.6783(4)	0.082(2)
C(31)	0.3100(2)	−0.2538(4)	0.7041(5)	0.049(2)
O(31)	0.3266(2)	−0.2812(4)	0.5996(4)	0.078(2)
C(32)	0.2203(2)	−0.3239(4)	0.9621(5)	0.049(2)
O(32)	0.1822(2)	−0.3899(3)	1.0052(4)	0.078(2)
C(33)	0.3689(3)	−0.3076(4)	0.9434(6)	0.060(2)
O(33)	0.4200(2)	−0.3634(4)	0.9856(6)	0.114(3)
P(1)	0.22363(5)	0.20507(9)	1.0437(1)	0.0331(4)
C(111)	0.1403(2)	0.2813(4)	1.1550(4)	0.034(2)
C(112)	0.0903(2)	0.3930(4)	1.1020(5)	0.045(2)
C(113)	0.0260(2)	0.4427(4)	1.1925(5)	0.057(2)
C(114)	0.0114(2)	0.3811(5)	1.3327(5)	0.059(2)
C(115)	0.0620(3)	0.2706(5)	1.3862(5)	0.058(2)
C(116)	0.1259(2)	0.2206(4)	1.2976(4)	0.046(2)
C(121)	0.2968(2)	0.2233(4)	1.1009(4)	0.037(2)
C(122)	0.3673(2)	0.1431(4)	1.0768(5)	0.050(2)
C(123)	0.4229(3)	0.1655(5)	1.1098(6)	0.069(3)
C(124)	0.4101(3)	0.2675(5)	1.1679(6)	0.066(3)
C(125)	0.3405(3)	0.3482(4)	1.1922(5)	0.056(2)
C(126)	0.2843(2)	0.3264(4)	1.1591(4)	0.044(2)
C(0)	0.2255(2)	0.3208(3)	0.8708(4)	0.035(2)
P(2)	0.28576(6)	0.2592(1)	0.7184(1)	0.0362(4)
C(211)	0.2472(2)	0.3864(4)	0.5762(4)	0.041(2)
C(212)	0.1938(2)	0.3740(4)	0.5254(4)	0.048(2)
C(213)	0.1622(3)	0.4744(4)	0.4238(5)	0.056(2)
C(214)	0.1819(3)	0.5887(5)	0.3738(5)	0.069(3)
C(215)	0.2350(4)	0.6007(5)	0.4231(6)	0.080(3)
C(216)	0.2675(3)	0.5022(4)	0.5246(5)	0.061(2)
C(221)	0.3727(2)	0.2923(4)	0.6925(5)	0.045(2)
C(222)	0.3859(3)	0.3583(5)	0.7705(5)	0.057(2)
C(223)	0.4531(3)	0.3821(6)	0.7421(6)	0.077(3)
C(224)	0.5075(3)	0.3415(6)	0.6343(8)	0.099(4)
C(225)	0.4947(3)	0.2791(7)	0.5525(8)	0.112(4)
C(226)	0.4277(3)	0.2534(6)	0.5820(6)	0.080(3)
C(1)	0.1079(2)	0.1527(4)	0.8658(4)	0.039(2)
O(101)	0.0525(2)	0.0992(3)	0.9179(4)	0.071(2)
O(102)	0.0979(2)	0.2688(3)	0.8272(4)	0.061(2)
C(101)	−0.0194(3)	0.1878(5)	0.9224(8)	0.101(4)
C(2)	0.1782(2)	0.0512(3)	0.8722(4)	0.033(2)
C(3)	0.1987(2)	−0.0503(3)	0.8060(4)	0.034(2)
C(4)	0.1568(2)	−0.0403(4)	0.7030(5)	0.046(2)

Table 5 (continued)

Atom	x	y	z	U_{eq} (Å^2)
O(401)	0.1415(2)	−0.1503(3)	0.7220(4)	0.072(2)
O(402)	0.1358(2)	0.0557(4)	0.6163(4)	0.091(2)
C(401)	0.0973(4)	−0.1498(7)	0.6336(8)	0.107(5)
H(12)	0.314(2)	0.014(4)	0.914(4)	0.07(1)
H(13)	0.244(2)	−0.166(4)	1.040(4)	0.05(1)

gave ten coloured bands and a brown baseline. Band 1 (red, R_f 0.57) was crystallised (CH_2Cl_2/MeOH) to give red crystals of $Ru_3\{\mu_3\text{-}PPhCH_2PPh(C_6H_4)\}(CO)_9$ (**4**) (29 mg, 18%), identified by IR and spot TLC. Band 4 (orange-yellow, R_f 0.47) was crystallised (CH_2Cl_2/MeOH) to give orange-red crystals of $Ru_4(\mu_3\text{-}H)\{\mu_4\text{-}C_2(CO_2Me)_2\}\{\mu\text{-}PPh_2CH_2PPh(C_6H_4)\}(CO)_9$ (**10**) (1 mg, 1%). IR: ν(CO) (cyclohexane) 2077 vs, 2044 vs, 2028 vs, 2016 w, 2001 m, 1988 s, 1959 w, 1948 w cm^{-1}. FAB MS: 1183, $[M-H]^+ \equiv [M']^+$, 11; 1155, $[M'-CO]^+$, 28; 1127, $[M'-2CO]^+$, 58; 1099, $[M'-3CO]^+$, 78; 1071, $[M'-4CO]^+$, 39; 1043, $[M'-5CO]^+$, 100; 1041, $[M'-C_2(CO_2Me)_2]^+$, 86; 1015, $[M'-6CO]^+$, 89; 1013, $[M'-CO-C_2(CO_2Me)_2]^+$, 86; 987, $[M'-7CO]^+$, 67; 985, $[M'-2CO-C_2(CO_2Me)_2]^+$, 56, 957, $[M'-3CO-C_2(CO_2Me)_2]^+$, 58; 929, $[M'-4CO-C_2(CO_2Me)_2]^+$, 53; 901, $[M'-5CO-C_2(CO_2Me)_2]^+$, 39. Band 5 (yellow, R_f 0.44) gave orange crystals (from CH_2Cl_2/MeOH) or $Ru_3(\mu\text{-}H)_2\{\mu_3\text{-}C_2(CO_2Me)_2\}(\mu\text{-}dppm)(CO)_7$ (**9**) (1 mg, 1%), identified by IR. Band 6 (purple, R_f 0.43) gave purple crystals (from CH_2Cl_2/MeOH) of $Ru_4\{\mu_4\text{-}C_2(CO_2Me)_2\}(\mu\text{-}dppm)(CO)_{10}$ (**11**) (4 mg, 2%). IR: ν(CO) (cyclohexane) 2071 s, 2039 vs, 2014 vs, 2001 s, 1999 (sh), 1969 w, 1963 (sh), 1949 w cm^{-1}. ^{1}H NMR: $\delta(CDCl_3)$ 3.03 (s, 3H, OMe), 3.79 (s, 3H, OMe), 4.75 (dt, $J(HH) = 14$, $J(PH) = 11$, 1H, CH_2), 4.97 (dt, $J(HH) = 14$, $J(PH) = 11$, 1H, CH_2), 6.92–7.83 (m, 20H, Ph). FAB MS: 1212, M^+, 27; 1181, $[M-OMe]^+$, 17; 1156, $[M-2CO]^+$, 29; 1128, $[M-3CO]^+$, 100; 1100, $[M-4CO]^+$, 96; 1072, $[M-5CO]^+$, 23; 1044, $[M-6CO]_+$, 100; 1016, $[M-7CO]^+$, 92; 988, $[M-8CO]^+$, 38; 986, $[M-3CO-CO_2Me]^+$, 46; 960, $[M-9CO]^+$, 35; 958, $[M-4CO-CO_2Me]^+$, 932, $[M-10CO]^+$, 35; 901, $[M-10CO-OMe]^+$, 32; 872, $[M-7CO-CO_2Me]^+$, 47. Band 7 (purple, R_f 0.40) was crystallised from CH_2Cl/hexane to give purple crystals of $Ru_3\{\mu_3\text{-}C_2(CO_2Me)_2\}(\mu\text{-}dppm)(\mu\text{-}CO)(CO)_7$ (**7**) (2 mg, 1%), identified by IR. Band 10 (olive-green, R_f 0.16) contained $Ru_3\{\mu_3\text{-}C_4(CO_2Me)_4\}(\mu\text{-}dppm)(CO)_6$ (**8**) (40 mg, 19%), identified by IR.

Alternative preparation of $Ru_3\{\mu_3\text{-}C_4(CO_2Me)_4\}(\mu\text{-}dppm)(CO)_6$ (8)

A mixture of $Ru_3\{\mu_3\text{-}C_2(CO_2Me)_2\}(\mu\text{-}dppm)(\mu\text{-}CO)(CO)_6$ (31 mg, 0.029 mmol) and $C_2(CO_2Me)_2$ (10 mg, 0.07 mmol) in CH_2Cl_2 (15 ml) was refluxed for 4.5 h; no starting material remained after this time. Crystallisation (CH_2Cl_2/MeOH) gave green crystals of $Ru_3\{\mu_3\text{-}C_4(CO_2Me)_4\}(\mu\text{-}dppm)(CO)_6$ (26 mg, 79%), identified by IR and spot TLC.

Preparation of $Ru_3(\mu\text{-}H)_2\{\mu_3\text{-}C_2(CO_2Me)_2\}(\mu\text{-}dppm)(CO)_7$ (9)

Hydrogen was passed through a solution of $Ru_3\{\mu_3\text{-}C_2(CO_2Me)_2\}(\mu\text{-}dppm)(\mu\text{-}CO)(CO)_6$ (24 mg, 0.023 mmol) in refluxing CH_2Cl_2 (20 ml) for 6 h. The solution was filtered through a cotton-wool plug, evaporated and the residue was crys-

Table 6

Non-hydrogen atomic coordinates and isotropic thermal parameters for $Ru_4(\mu_3\text{-}H)\{\mu_4\text{-}C_2(CO_2Me)_2\}\{\mu\text{-}PPh_2CH_2PPh(C_6H_4)\}(CO)_9$ (**10**)

Atom	x	y	z	U (Å^2)
Ru(1)	0.08583(6)	0.64626(3)	0.07526(2)	0.0298(3)
Ru(2)	0.21726(6)	0.76684(3)	0.13487(2)	0.0285(3)
Ru(3)	0.37439(6)	0.68450(4)	0.06057(2)	0.0355(4)
Ru(4)	0.17234(7)	0.70306(4)	−0.01849(2)	0.0376(4)
C(11)	0.1045(8)	0.5356(5)	0.0656(3)	0.044(5)
O(11)	0.1207(6)	0.4703(3)	0.0580(2)	0.064(4)
C(12)	−0.1012(8)	0.6422(5)	0.0512(3)	0.046(5)
O(12)	−0.2144(6)	0.6378(4)	0.0394(3)	0.065(4)
C(21)	0.3206(8)	0.8472(5)	0.1650(3)	0.041(5)
O(21)	0.3852(6)	0.8975(3)	0.1828(2)	0.062(4)
C(31)	0.4994(8)	0.7146(5)	0.1172(3)	0.049(5)
O(31)	0.5845(6)	0.7328(4)	0.1478(3)	0.072(4)
C(32)	0.4926(9)	0.7120(6)	0.0056(3)	0.058(6)
O(32)	0.5647(6)	0.7250(5)	−0.0270(2)	0.080(5)
C(33)	0.4320(8)	0.5770(5)	0.0589(3)	0.050(5)
O(33)	0.4611(7)	0.5120(4)	0.0585(3)	0.082(5)
C(41)	0.2010(9)	0.5992(5)	−0.0388(3)	0.050(5)
O(41)	0.2211(7)	0.5371(4)	−0.0534(2)	0.070(4)
C(42)	−0.002(1)	0.7149(5)	−0.0550(3)	0.058(6)
O(42)	−0.1038(7)	0.7232(5)	−0.0782(3)	0.100(6)
C(43)	0.2565(9)	0.7518(5)	−0.0756(3)	0.051(5)
O(43)	0.3000(8)	0.7759(4)	−0.1144(3)	0.082(5)
P(1)	0.0215(2)	0.6370(1)	0.16214(8)	0.031(1)
C(111)	−0.0858(8)	0.5536(4)	0.1764(3)	0.040(5)
C(112)	−0.0292(9)	0.4785(5)	0.1768(3)	0.049(5)
C(113)	−0.112(1)	0.4121(5)	0.1826(4)	0.071(7)
C(114)	−0.248(1)	0.4221(6)	0.1874(4)	0.078(7)
C(115)	−0.305(1)	0.4954(7)	0.1873(4)	0.081(8)
C(116)	−0.2237(9)	0.5618(6)	0.1820(4)	0.061(6)
C(121)	0.1632(7)	0.6386(4)	0.2118(3)	0.031(4)
C(122)	0.2563(7)	0.7005(4)	0.2034(3)	0.031(4)
C(123)	0.3634(8)	0.7097(5)	0.2415(3)	0.041(4)
C(124)	0.3782(9)	0.6588(5)	0.2848(3)	0.054(5)
C(125)	0.2857(9)	0.5995(5)	0.2922(3)	0.053(5)
C(126)	0.1786(8)	0.5885(4)	0.2555(3)	0.041(5)
C(0)	−0.0786(7)	0.7229(4)	0.1808(3)	0.037(4)
P(2)	0.0389(2)	0.8066(1)	0.18205(7)	0.031(1)
C(211)	−0.0628(7)	0.8911(4)	0.1604(3)	0.037(4)
C(212)	−0.1950(9)	0.8996(5)	0.1771(3)	0.051(5)
C(213)	−0.2701(9)	0.9650(6)	0.1631(4)	0.069(7)
C(214)	−0.216(1)	1.0234(6)	0.1332(5)	0.077(7)
C(215)	−0.085(1)	1.0170(5)	0.1167(4)	0.064(6)
C(216)	−0.0081(8)	0.9497(5)	0.1303(3)	0.049(5)
C(221)	0.0744(7)	0.8305(4)	0.2520(3)	0.033(4)
C(222)	0.1200(8)	0.9056(4)	0.2656(3)	0.041(5)
C(223)	0.1529(8)	0.9246(5)	0.3183(3)	0.049(5)
C(224)	0.1430(9)	0.8715(5)	0.3573(3)	0.055(6)
C(225)	0.0994(9)	0.7962(5)	0.3445(3)	0.053(5)
C(226)	0.0646(8)	0.7766(5)	0.2929(3)	0.044(5)
O(101)	−0.1224(5)	0.8039(3)	0.0557(2)	0.047(3)
O(102)	0.0116(6)	0.8816(3)	0.0104(2)	0.060(4)

Table 6 (continued)

Atom	x	y	z	U (Å^2)
C(101)	−0.234(1)	0.8540(8)	0.0368(6)	0.12(1)
C(1)	−0.0042(8)	0.8248(5)	0.0380(3)	0.048(5)
C(2)	0.1078(7)	0.7678(4)	0.0545(3)	0.035(4)
C(3)	0.2484(8)	0.7856(4)	0.0499(3)	0.039(4)
C(4)	0.3059(8)	0.8628(5)	0.0296(3)	0.050(5)
O(401)	0.2924(7)	0.9190(3)	0.0651(2)	0.066(4)
O(402)	0.3689(8)	0.8735(4)	−0.0094(3)	0.083(5)
C(401)	0.358(2)	0.9932(7)	0.0553(5)	0.13(1)
H	0.246(6)	0.653(4)	0.108(2)	0.3(2)

tallised (CH_2Cl_2/MeOH) to give orange crystals of $Ru_3(\mu\text{-}H)_2\{\mu_3\text{-}C_2(CO_2Me)_2\}(\mu\text{-dppm})(CO)_7$ (**9**) (18 mg, 77%), m.p. > 180°C (dec.). (Found: C, 44.12; H, 2.98; M (mass spectrometry), 1029; $C_{38}H_{30}O_{11}P_2Ru_3$ calc.: C, 44.41; H, 2.94%; M, 1029). IR: ν(CO) (cyclohexane) 2072 vs, 2043 s, 2019 vs, 2004 vs, 1998 (sh), 1969 w (br), 1966 (sh) cm^{-1}. ^1H NMR: $\delta(CDCl_3)$ −19.22 (d, J(PH) = 39, 1H, Ru-H), −14.89 (t, J(PH) = 14, 1H, Ru-H), 3.46 (s, 3H, OMe), 3.56 (m, part of ABXY pattern, 1H, CH_2), 3.76 (s, 3H, OMe), 4.49 (m, part of ABXY pattern, 1H, CH_2), 6.96–7.54 (m, 20H, Ph). Minor peaks were observed at −20.76 (t, J(PH) = 17, Ru-H), −15.78 (t, J(PH) = 14, Ru-H), 3.29 (s, OMe), 4.67 (m, CH_2). FAB MS: 1029, M^+, 30; 998, $[M - OMe]^+$, 52; 972, $[M - H - 2CO]^+$, 35; 945, $[M - 3CO]^+$, 80; 917, $[M - 4CO]^+$, 100; 887, $[M - C_2(CO_2Me)_2]^+$, 83; 859, $[M - CO - C_2(CO_2Me)_2]^+$, 64.

Reaction between $Ru_3(\mu_3\text{-}PPhCH_2PPh(C_6H_4))\}(CO)_9$ and $C_2(CO_2Me)_2$

The alkyne (2 ml of a 0.26M solution in tetrahydrofuran, 0.52 mmol) was added to $Ru_3\{\mu_3\text{-}PPhCH_2PPh(C_6H_4)\}(CO)_9$ (100 mg, 0.116 mmol) dissolved in the same solvent (20 ml). The mixture was heated at reflux point for 135 min, after which time solvent was removed and four products were separated by radial chromatography (silica gel; acetone/light petroleum 1/4). Band 3 (green) was crystallised from CH_2Cl_2/MeOH to give dark green crystals of $Ru_3\{\mu_3\text{-}PPhCH_2PPh(C_6H_4)\}\{\mu\text{-}C_4(CO_2Me)_4\}(CO)_6$ (**12**) (26 mg, 21%), m.p. > 150°C (dec.). (Found: C, 41.80; H, 2.62; M (mass spectrometry), 1063; $C_{37}H_{28}O_{14}P_2Ru_3$ calc.: C, 41.86; H, 2.66%; M, 1063). IR: ν(CO) (cyclohexane) 2066 m, 2050 vs, 2025 s, 2009 m, 1989 w, 1977 m cm^{-1}; IR (Nujol): ν(CO) 2062 m, 2046 vs, 2020 s, 2002 s, 1992 m, 1978 s, 1969 s; ν(C=O) 1727 (sh), 1718 m, 1708 m, 1700 (sh); ν(COO) 1238 m, 1214 m, 1205 m, 1178 m, 1172 m cm^{-1}. ^1H NMR: $\delta(CDCl_3)$ 2.49–3.06 (m, part of ABXY pattern, 2H, CH_2), 3.45, 3.63, 3.88, 3.91 (each s, 3H, OMe), 6.29–8.04 (m, 14H, Ph + C_6H_4). FAB MS: 1063, M^+, 7; 1035, $[M - CO]^+$, 26; 1007, $[M - 2CO]^+$, 16; 979, $[M - 3CO]^+$, 100; 951, $[M - 4CO]^+$, 34; 923, $[M - 5CO]^+$, 44; 921, $[M - C_2(CO_2Me)_2]^+$, 44; 895, $[M - 6CO]^+$, 12; 893, $[M - CO - C_2(CO_2Me)_2]^+$, 12; 865, $[M - 2CO - C_2(CO_2Me)_2]^+$, 11. The other three bands contained complexes which have not identified.

Crystallography

Unique data sets were measured at *ca.* 295 K within the specified $2\theta_{max}$ limits using an Enraf-Nonius CAD4 diffractometer ($2\theta/\theta$ scan mode; monochromatic

Table 7

Crystal data and refinement details for **8**, **9** and **10**

	8	**9**	**10**
Formula	$C_{43}H_{34}O_{14}P_2Ru_3$	$C_{38}H_{30}O_{11}P_2Ru_3$	$C_{40}H_{28}O_{13}P_2Ru_4$
MW	1139.9	1027.8	1182.9
Crystal system	Triclinic	Triclinic	Monoclinic
Space group	$P\bar{1}$ (No. 2)	$P\bar{1}$ (No. 2)	$P2_1/n$ (No. 14)
a, Å	18.676(4)	19.932(9)	9.789(4)
b, Å	12.010(2)	11.289(2)	17.007(10)
c, Å	10.882(3)	10.236(3)	25.094(10)
α, deg.	67.37(2)	71.13(2)	–
β, deg.	86.20(2)	72.43(3)	93.27(3)
γ, deg.	79.91(2)	70.19(3)	–
U, Å^3	2218	2002	4171
Z	2	2	4
D_c, g cm^{-3}	1.71	1.70	1.89
$F(000)$	1132	1016	2312
Crystal size, mm	0.35×0.25×0.26	0.15×0.05×0.25	0.16×0.23×0.16
A^* (min, max)	1.34, 1.48	1.06, 1.16	1.14, 1.20
μ, cm^{-1}	12.1	11.2	14.0
$2\theta_{max}$, deg.	65	55	50
N	16017	9065	7344
N_0	14020	6426	5352
R	0.024	0.031	0.039
R_w	0.031	0.031	0.046

Mo-K_α radiation, λ 0.7107$_3$ Å); N independent reflections were obtained, N_o with $I > 3\sigma(I)$ being considered 'observed' and used in the full matrix least squares refinements after gaussian absorption correction. Anisotropic thermal parameters were refined for the non-hydrogen atoms; $(x, y, z, U_{iso})_H$ were included constrained at estimated values (but see below). Conventional residuals R, R' on $|F|$ are quoted, statistical weights derivative of $\sigma^2(I) = \sigma^2(I_{diff}) + 0.0004\sigma^4(I_{diff})$ being used. Computation used the XTAL 2.6 program system [21] implemented by S.R. Hall; neutral atom complex scattering factors were employed. Crystal data and refinement details are summarised in Table 7. Pertinent results are given in the Figure and Tables. Lists of structure factor amplitudes, thermal and hydrogen atom parameters, and full non-hydrogen geometries are available from the authors. Abnormal features/variations in procedure were as follows: **8**. All hydrogen atoms were located and refined in (x, y, z, U_{iso}); **9**. Core hydrogen atoms H(12, 13) were located and refined in (x, y, z, U_{iso}); **10**. The core hydrogen atom was located and refined in (x, y, z, U_{iso}).

Acknowledgments

We thank the Australian Research Council for financial support and Johnson Matthey Technology Centre for a generous loan of $RuCl_3 \cdot nH_2O$. PAH held a University of Adelaide Post-graduate Scholarship.

References

1 Part LXXX: C.J. Adams, M.I. Bruce, B.W. Skelton and A.H. White, J. Organomet. Chem, 430 (1992) 181.

2 F.A. Cotton and B.E. Hanson, Inorg. Chem., 16 (1977) 3369.

3 A.W. Coleman, D.F. Jones, P.H. Dixneuf, C. Brisson, J.-J. Bonnet and G. Lavigne, Inorg. Chem., 23 (1984) 952.

4 N. Lugan, J.-J. Bonnet and J.A. Ibers, J. Am. Chem. Soc., 107 (1985) 4484.

5 (a) M.I. Bruce, O. bin Shawkataly and M.L. Williams, J. Organomet. Chem., 287 (1985) 127; (b) M.I. Bruce, E. Horn, O. bin Shawkataly, M.R. Snow, E.R.T. Tiekink and M.L. Williams, J. Organomet. Chem., 316 (1986) 187.

6 M.I. Bruce, P.A. Humphrey, B.W. Skelton, A.H. White and M.L. Williams, Aust. J. Chem., 38 (1985) 1301.

7 D.F. Foster, J. Harrison, B.S. Nicholls and A.K. Smith, J. Organomet. Chem., 295 (1985) 99.

8 B. Ambwani, S.K. Chawla and A.J. Poë, Inorg. Chem., 24 (1985) 2635; idem, Inorg. Chim. Acta, 133 (1987) 93; idem, Polyhedron, 7 (1988) 1939.

9 P. Fompeyrine, G. Lavigne and J.-J. Bonnet, J. Chem. Soc., Dalton Trans., (1987) 91.

10 M.I. Bruce, J.G. Matisons, B.W. Skelton and A.H. White, J. Organomet. Chem., 251 (1983) 249.

11 M.I. Bruce, P.A. Humphrey, B.W. Skelton and A.H. White, J. Organomet. Chem., 417 (1991) 431.

12 S. Rivomanana, G. Lavigne, N. Lugan, J.-J. Bonnet, R. Yanez and R. Mathieu, J. Am. Chem. Soc., 111 (1989) 8959.

13 K.I. Hardcastle, T. McPhillips, A.J. Arce, Y. De Sanctis, A.J. Deeming and N.I. Powell, J. Organomet. Chem., 389 (1990) 361.

14 J.A. Clucas, D.F. Foster, M.M. Harding and A.K. Smith, J. Chem. Soc., Chem. Commun., (1984) 949.

15 D.M.P. Mingos and A.S. May in D.F. Shriver, H.D. Kaesz and R.D. Adams, (Eds.), The Chemistry of Metal Cluster Complexes, VCH, New York, 1990, p. 11.

16 M.I. Bruce, P.A. Humphrey, B.W. Skelton and A.H. White, unpublished results.

17 M.R. Churchill, T.S. Janik, T.P. Duggan and J.B. Keister, Organometallics, 6 (1987) 799.

18 G. Predieri, A. Tiripicchio, M. Tiripicchio-Camellini, M. Costa and E. Sappa, Organometallics, 9 (1990) 1729.

19 F. Muller, I.M. Han, G. van Koten, K. Vrieze, D. Heijdenrijk, R.L. de Jong and M.C. Zoutberg, Inorg. Chim. Acta, 158 (1989) 81.

20 M.I. Bruce, B.K. Nicholson and M.L. Williams, Inorg. Synth., 26 (1989) 276; 28 (1990) 225.

21 S.R. Hall and J.M. Stewart (Eds.), XTAL Users' Manual, Version 2.6, Universities of Western Australia and Maryland, 1988.